

A CODED APERTURE IMAGING SYSTEM  
OPTIMIZED FOR HARD X-RAY AND GAMMA RAY ASTRONOMY

N. Gehrels<sup>1</sup>, T. L. Cline<sup>1</sup>, A. F. Hutters<sup>3</sup>,  
M. Leventhal<sup>2</sup>, C. J. MacCallum<sup>3</sup>, J. D. Reber<sup>1,4</sup>,  
P. D. Stang<sup>3</sup>, B. J. Teegarden<sup>1</sup>, and J. Tueller<sup>1</sup>

1. NASA/Goddard Space Flight Center, Greenbelt, MD 20771
2. AT&T Bell Laboratories, Murray Hill, NJ 07974
3. Sandia National Laboratories, Albuquerque, NM 87185
4. SUNY/Geneseo, NY 14454

ABSTRACT

A coded aperture imaging system has been designed for the Gamma-Ray Imaging Spectrometer (GRIS). The system is optimized for imaging 511-keV positron-annihilation photons. For a galactic center 511-keV source strength of  $10^{-3} \text{ cm}^{-2}\text{s}^{-1}$ , the source location accuracy is expected to be  $\pm 0.2^\circ$ .

1. Introduction Current gamma-ray spectrometers observing in the 70 keV to 10 MeV nuclear-line energy range have poor source localization capabilities. They typically have broad fields of view ( $\sim 10^\circ$  FWHM) and no imaging systems. Recent discoveries of a number of gamma-ray sources with lines in their spectra (1,2,3) have increased interest in building spectrometers capable of mapping the source regions. An example is the positron annihilation line at 511 keV from the direction of the galactic center, whose location is known only to within  $\pm 4^\circ$  (4). This large error circles several galactic-center X-ray sources in addition to the compact radio source Sgr A near the dynamic center of the galaxy. Localizing the line emission is currently one of the major goals in gamma-ray line astronomy.

The most promising technique for mapping in this energy range is coded aperture imaging using Uniformly Redundant Arrays (URAs). The basic idea is to place an array of blocking elements in the instrument aperture whose pattern is chosen such that the shadows cast on the detectors by sources at different locations in the field of view (FOV) give linearly independent sets of detector signals (5). The signals measured during an observation can then be uniquely deconvolved to give maps of the sky. Several papers have been written (6-10) discussing the application of coded aperture imaging to low-energy gamma-ray astronomy.

We are currently building a balloon-borne spectrometer to be flown in fall 1986 called the Gamma-Ray Imaging Spectrometer (GRIS) that will have a URA imaging system. In this paper we describe the imaging system and present the results of laboratory and computer simulations of its performance. A general description of the GRIS instrument is given in a companion paper (11).

2. Description of the Imaging System The Ge detectors in the GRIS instrument are located in every other cell of a 7.5 cm lattice as shown in Figure 1. The mask is a URA with a 3x5 element unit cell. It is located 1.5 m above the detectors and is arranged on a 7.5 cm grid. The

opaque elements are individual NaI blocks 6.8 cm square by 7.6 cm thick, each viewed by its own photomultiplier tube. Calculations and simulations we performed during the instrument design phase showed that it was essential for the mask to be active in order to achieve low levels for the instrumental line background at 511 keV and the continuum background over the entire spectrum.

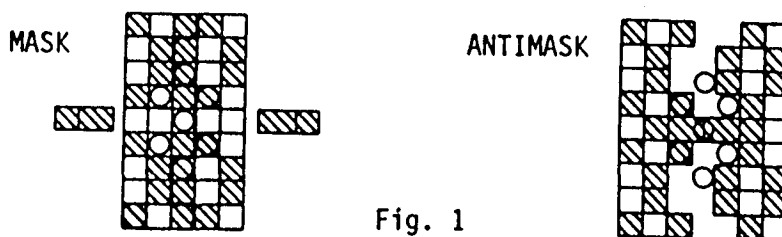


Fig. 1

Another feature of the GRIS imaging system that is essential for high-background observations is the ability to alternate between mask and antimask (see, e.g., ref. 7). The antimask is the complement of the mask, having opaque elements where the mask is open and vice versa. The incident gamma-ray flux is therefore square-wave modulated by the alternation, which is the optimum modulation for background subtraction. Normally mask-antimask systems have a separate structure for both the mask and antimask, each of which move in and out of the field of view. By a novel technique that reduces instrument weight and size, the GRIS mask is itself converted into its own antimask as illustrated in Figure 1. The mask divides into halves while two independent elements rotate into the center.

Both the mask and antimask also move as units left and right one cell so that a detector is located under each of the 15 elements in the mask unit cell at least once. In this way the 7-detector GRIS array is made to act like a 15-detector array in terms of its imaging capability. To produce a map, the mask system moves through 6 positions (3 mask, 3 antimask).

The maps produced by the imaging system have 15 sky bins arranged in a 3x5 matrix. The bins are each  $3^\circ$  square as determined by the mask cell size and the detector-mask separation. The region mapped is therefore  $9^\circ \times 15^\circ$ . As will be shown below, this bin size and mapping region are a good match for the hard X-ray source distribution in the galactic center direction.

**3. Imaging Sensitivity and Resolution** There is a decrease in sensitivity that all imaging systems suffer compared with non-imaging wide FOV systems which occurs when a source is not in the center of a sky bin. This is due to the fact that the source signal in the detectors is not fully modulated. The effect can be as large as a factor of 2.2 in sensitivity if the source is at the corner of four bins. To reduce this variation in sensitivity across the map and also increase the number of effective pixels in the final map, we will use an offset pointing technique. The basic idea is that the pointing direction of the instrument is changed between imaging cycles so that a given source appears at

different locations in the different sky maps. By changing the pointing  $1^\circ$  at a time in a  $3 \times 3$  grid, the  $3^\circ$  sky bins are divided into  $1^\circ$  pixels. The final map then has an approximately uniform sensitivity that turns out for a single point source to be  $\sim 1.4$  times poorer than a wide FOV instrument. The  $3^\circ$  bin size combined with the finite detector size gives the imaging system a point-spread function FWHM of  $\sim 4^\circ$ .

The localization accuracy of the centroid of a point source image depends on the source strength and the number of sources in the field, but is in general much better than the  $4^\circ$  beam width. For the GRIS mask and detector arrangement operated in the offset pointing mode, the accuracy to which the position of a point source of strength  $S$  (photons  $\text{cm}^{-2}\text{s}^{-1}$ ) can be determined is given by

$$\text{source location accuracy } (1\sigma) \approx 1.4 \theta \frac{\sigma_S}{S} \quad (1)$$

where  $\theta$  is the bin size of the mask ( $3^\circ$ ), and  $\sigma_S$  is the uncertainty in the flux measurement that would occur for a wide FOV observation. For a galactic center 511-keV line flux of  $10^{-3}$   $\text{ph cm}^{-2}\text{s}^{-1}$  observed by GRIS for 8 hours at  $3.5 \text{ g cm}^{-2}$  atmosphere depth from Alice Springs, Australia, the value of  $\sigma_S/S$  is better than  $1/20$ . Hence, GRIS will be able to localize the source position to within  $\pm 0.2^\circ$ , which will be more than an order of magnitude improvement over the present best position (4).

4. Laboratory Tests and Computer Simulations A special laboratory test setup of the GRIS imaging system was assembled using NaI detectors in place of the Ge array and Fe and Al mask elements in place of the NaI elements. The detector and mask geometries were similar to those of GRIS except that the laboratory detector-mask separation was 45 cm instead of 1.5 m. This gives  $9^\circ$  sky bins, and was done to reduce the effects of the nonparallel gamma-ray beam produced by the radioactive source used in the laboratory. An  $^{241}\text{Am}$  source was located 10 m from the detectors on a large, precise x-y positioning system. Figure 2 shows a map generated in the laboratory of a single on-axis source. The 9 offset pointing maps were combined into a final map with  $3^\circ$  pixel size (three times GRIS). The laboratory data were taken with very high statistical significance ( $\sim 1\%$ ) and then noise was added to the detector signals by computer. The noise level was chosen such that each unblocked detector signal was a  $1.7\sigma$  measurement. This corresponds to a measurement of total significance  $\sigma_S/S = 0.06$  in Equation (1).

To better understand the mapping capabilities of the GRIS imaging system, a computer simulation of the galactic center was performed. The computer simulation assumed a full 8-hour observation with GRIS of the 20-80 keV X-ray range from Alice Springs. Included in the galactic center direction were the 3 strongest sources (GX1+4, GCX-1, and GX5-1), with intensities assumed to be those measured by HEAO A4. In order to make the simulation as realistic as possible the data were "taken" using offset pointing, rotation of the image in the FOV, different length mask-antimask intervals during transit, and the expected instrumental background (12). Figure 3 shows the results, with the three sources clearly resolved.

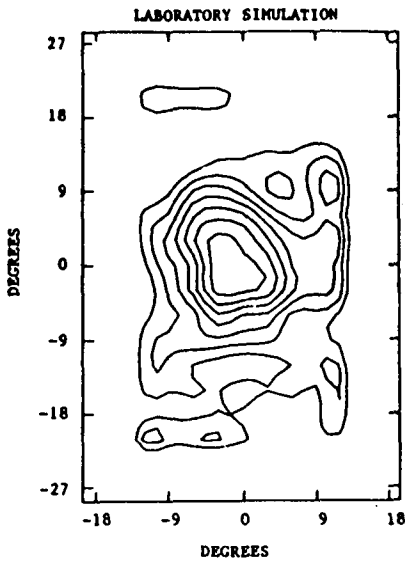


Fig. 2

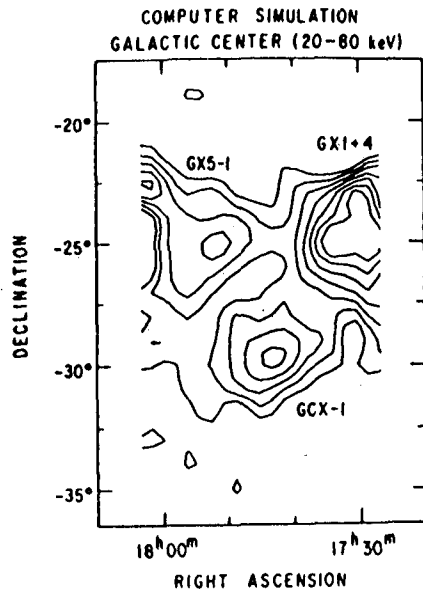


Fig. 3

### References

1. M. Leventhal, et al., *Ap. J.* 225, L11, 1978.
2. R. C. Lamb, et al., *Nature* 305, 37, 1983.
3. W. A. Mahoney, et al., *Ap. J.* 286, 578, 1984.
4. G. R. Riegler, et al., *Ap. J.* 248, L13, 1981.
5. E. E. Fenimore and T. M. Cannon, *Applied Optics* 17, 337, 1978.
6. G. Di Cocco, et al., *IEEE Trans. Nucl. Sci.* NS-31, No. 1, 771, 1984.
7. M. L. McConnell, et al., *IEEE Trans. on Nucl. Sci.* NS-29, No. 1, 155, 1982.
8. R. Kroeger and D. Muller, *18th ICRC, Vol. T*, 1, 1983.
9. J.-P. Roques and G. Debousy, *14th Inter. Symp. on Space Tech. and Sci.*, Tokyo, p. 1523, 1984.
10. W. R. Cook, et al., *IEEE Trans. Nucl. Sci.* NS-31, No. 1, 771, 1984.
11. B. J. Teegarden, et al., *19th ICRC*, 1985.
12. N. Gehrels, to be published in *Nucl. Inst. Meth.*, 1985.